Temperature effects on the electrical properties and structure of interfacial and bulk defects in Al/SiN x : H/Si devices

F. L. Martnez, E. San Andrés, A. del Prado, I. Mártil, D. Bravo, and F. J. López

Citation: Journal of Applied Physics **90**, 1573 (2001); doi: 10.1063/1.1380992
View online: http://dx.doi.org/10.1063/1.1380992
View Table of Contents: http://scitation.aip.org/content/aip/journal/jap/90/3?ver=pdfcov
Published by the AIP Publishing

Temperature effects on the electrical properties and structure of interfacial and bulk defects in Al/SiN_x:H/Si devices

F. L. Martínez, E. San Andrés, A. del Prado, and I. Mártil[a)]
Departamento de Física Aplicada III, Universidad Complutense de Madrid, E-28040 Madrid, Spain

D. Bravo and F. J. López
Departamento de Física de Materiales C-IV, Universidad Autónoma de Madrid, E-28049 Madrid, Spain

(Received 4 December 2000; accepted for publication 26 April 2001)

Bulk properties of SiN_x:H thin film dielectrics and interface characteristics of SiN_x:H/Si devices are studied by a combination of electrical measurements (capacitance–voltage and current–voltage characteristics) and defect spectroscopy (electron spin resonance). The SiN_x:H films were deposited by an electron cyclotron resonance plasma method and subjected to rapid thermal annealing postdeposition treatments at temperatures between 300 and 1050 °C for 30 s. It is found that the response of the dielectric to the thermal treatments is strongly affected by its nitrogen to silicon ratio (N/Si$=x$) being above or below the percolation threshold of the Si–Si bonds in the SiN_x:H lattice, and by the amount and distribution of the hydrogen content. The density of Si dangling bond defects decreases at moderate annealing temperatures (below 600 °C) in one order of magnitude for the compositions above the percolation threshold (nitrogen rich, $x=1.55$, and near stoichiometric, $x=1.43$). For the nitrogen rich films, a good correlation exists between the Si dangling bond density and the interface trap density, obtained from the capacitance measurements. This suggests that the observed behavior is mainly determined by the removal of states from the band tails associated to Si–Si weak bonds, because of the thermal relaxation of the bonding strain. At higher annealing temperatures the deterioration of the electrical properties and the increase of the Si dangling bonds seem to be associated with a release of trapped hydrogen from microvoids of the structure. For the silicon rich samples rigidity percolates in the network resulting in a rigid and strained structure for which the degradation phenomena starts at lower temperatures than for the other two types of samples. © *2001 American Institute of Physics.* [DOI: 10.1063/1.1380992]

I. INTRODUCTION

The electrical properties of silicon nitride thin films (SiN_x:H) have been the subject of intense research in several areas such as thin film transistors,[1] memory devices,[2] and inversion layer solar cells.[3] However, at the present time, the main point of concern is the potential application of SiN_x:H to the gate structure of complementary metal–oxide–semiconductor transistors.[4,5] This application is motivated by the continuous downscaling of the channel length below 180 nm, which is pushing the SiO_2 gate dielectric thickness below 2.0 nm. In this ultrathin range, boron transport from the p^+ poly-Si gate electrode to the channel region occurs during the high temperature anneals that are required to activate the B dopant atoms. Additionally, direct and Fowler–Nordheim tunneling currents[6] become important and comparable to off-state drain currents. The higher dielectric constant of SiN_x:H compared to SiO_2 allows increasing the physical thickness of the gate dielectric while retaining a low oxide equivalent thickness.[7]

Interfacial and bulk electrical properties of SiN_x:H have been investigated under a number of different approaches. Extensive studies exist about its defect structure, particularly about the identification and properties of the silicon[8,9] and nitrogen[10,11] dangling bonds by electron spin resonance (ESR).

On the other hand, the dominant mode of electronic conduction appears to be Poole–Frenkel emission[12] which, in the lower range of applied electric fields, turns over to an ohmic behavior.[13] For ultrathin films with a low density of defects, Fowler–Nordheim and direct tunneling conduction have been observed.[6,13] The studies of the SiN_x:H/Si interface have been performed mainly by capacitance–voltage ($C-V$) measurements,[12,14] from which the density of interface states can be calculated.[15–17] Much effort has been devoted to reduce this density of states to a level comparable to the Si/SiO_2 interface.

SiN_x:H thin films deposited by plasma assisted chemical vapor deposition methods generally contain a large amount of bulk and interfacial traps. These are attributed to the damage caused by energetic ions and electrons impinging on the growing surface during the deposition process. Significant reduction of these centers can be achieved by indirect plasma methods such as the remote plasma deposition technique[18] and the electron cyclotron resonance (ECR) method.[19] In these cases, the substrate is placed out of the plasma region and therefore is not subjected to direct plasma exposure. By any of these indirect techniques, the dielectric can be deposited directly on the silicon substrate at low temperature[18,19] without any previous interface conditioning process.

[a)]Electronic mail: imartil@eucmax.sim.ucm.es

TABLE I. Summary of characteristics obtained in previous works for the three types of films deposited for this study. The data of silicon and nitrogen content were determined by combined Rutherford backscattering and energy dispersive x-ray analysis, while the content of bonded hydrogen was calculated from the infrared spectra of the films.

Nitrogen to silane gas flow ratio (R)	Denomination	Ratio of nitrogen to silicon in the film (x)	RTA temperature onset for nitrogen loss	Bonded hydrogen	RTA temperature onset for bonded hydrogen loss
1	silicon rich	0.97 ± 0.03	600 °C	Si–H bonds predominate over N–H bonds	N–H bonds: 400 °C Si–H bonds: 500 °C
1.6	quasi stoichiometric	1.43 ± 0.02	700 °C	N–H bonds predominate over Si–H bonds	N–H bonds: 500 °C Si–H bonds: 700 °C
7.5	nitrogen rich	1.55 ± 0.04	No loss of nitrogen	Only N–H bonds are detected	900 °C

Concerning the application of SiN_x:H films to III–V compound semiconductor based technology, an interface control layer (ICL) or some kind of interface treatment becomes necessary due to the much higher instability of the surface of these materials. Notable success has been achieved with sulfur passivation,[20] CdS chemical baths,[21] and ICL of elemental silicon grown pseudomorphically on the substrate wafer.[22]

While the origin of bulk defects in SiN_x:H has been found to be dominated by silicon dangling bonds,[8,9] the physical nature of the interfacial states is not so well understood. These states usually exhibit a *U*-shaped distribution within the forbidden energy gap and are often ascribed to a background *U*-shaped continuum due to band-tail levels superimposed to localized peaks. Specific superficial defects such as the so-called P_b center would be the origin of the spectral peaks.[23,24] Other models for the interchange of charge at the interface have ascribed the density of states to deep levels in the SiN_x:H, in which electronic transitions take place by direct tunneling with the silicon bands.[25] These defects consist of a silicon dangling bond (*K* center) in which the three other bonds of the silicon atom may be saturated by nitrogen or silicon atoms in a proportion that depends on the composition of the SiN_x:H. Although charge carrier injection in silicon nitride/silicon junctions has been reported to occur from as far as 20 nm from the interface,[26] *K* centers should be located only a few nanometers from the interface in order to exchange charge with the silicon so rapidly that they can be viewed as interface state defects.

Another influence that must not be neglected in analyzing the structure of defects and the electrical properties is that of the hydrogen content of the film. Near neighbor Si–H and SiN–H groups linked through the H-bonding interaction may trap a thermally or optically generated hole and produce a metastable defect pair consisting on an overcoordinated nitrogen atom.[27] At the interface, H atoms bonded directly to Si atoms can form hydrogen bonds with N–H groups which act as precursor sites for defect generation.[28] On the other hand, H atoms compensate what otherwise would be Si dangling bond defects, and thereby contribute to decreased levels of interface trapping states.[28] Generally, it has been accepted that the presence of hydrogen is beneficial for the application of SiN_x:H to thin film transistor gate dielectrics because it reduces the number of constraints. In this way, it makes possible an average coordination number very similar to that of SiO_2. On the contrary, for field effect applications, the negative effects of hydrogen as a precursor of defect generation are often found to predominate. In this case thermal annealing postdeposition treatments have been applied to reduce the amount of bonded and nonbonded hydrogen while at the same time promoting the formation of Si–N bonds.[27,29]

In this article, we will analyze the effects of rapid thermal annealing processes (RTA) on the electrical properties of ECR plasma deposited SiN_x:H thin film dielectrics in metal–nitride–silicon (MNS) structures. It will be shown that the changes induced by the RTA treatments on the results of the electrical measurements can be correlated to the density of paramagnetic Si dangling bonds detected by ESR.

II. EXPERIMENT

SiN_x:H thin films of variable composition were deposited by an ECR plasma method directly on silicon wafers. The deposition reactor was an Astex 4500 machine operating at 2.45 GHz and 100 W of microwave power. The wafers had been previously sliced in square pieces of 0.5 cm of side and subjected to organic solvents and dilute HF cleaning in a glove chamber with inert gas purge before their introduction in the plasma system. The purged cleaning chamber coupled to the entrance port of the vacuum system avoided exposure of the wafer surface to air after the last step of the cleaning process and therefore prevented oxidation of the hydrogen terminated surface. This ensured that the SiN_x:H film was deposited directly on the silicon surface without an intermediate oxide layer. The composition of the SiN_x:H was controlled by the nitrogen to silane gas flow ratio ($\mathbf{R}=N_2/SiH_4$). Three values of **R** were used ($\mathbf{R}=1$, 1.6, and 7.5), which resulted in three compositions (defined in this article by the nitrogen to silicon ratio, $x=N/Si$) with characteristic properties and response to the thermal treatments. In Table I we summarize some of these characteristics obtained in our previous studies by combined Rutherford backscattering and energy dispersive x-ray analysis (RBS/EDX) together with infrared spectroscopy.[30] In the following, we will refer to the three types of samples analyzed as Si rich ($\mathbf{R}=1$; $x=0.97$), near stoichiometric ($\mathbf{R}=1.6$; $x=1.43$) and N rich ($\mathbf{R}=7.5$; $x=1.55$).

For the ESR measurements, thick films were needed to obtain a good signal to noise ratio. However, the higher thickness that can be grown is limited by the internal stress of the SiN_x:H film, which produces loss of adherence and

film peeling for thickness values above a certain limit that depends on the composition. The stress and rigidity of the SiN_x:H network is increased as the film becomes increasingly Si rich, so the maximum allowed film thickness is reduced by the higher Si content. The thickness of the films grown for the ESR measurements were 640 nm for the N-rich samples, 480 nm for the near stoichiometric, and 200 nm for the Si rich. The silicon wafers had a (111) orientation and 80 Ω cm resistivity, and the substrate holder was not intentionally heated during deposition.

For the electrical measurements on MNS capacitors, the thickness of the SiN_x:H film ranged between 30 and 40 nm for the three compositions, and the substrate was heated to 200 °C during the deposition process. In this case the wafers had a (100) orientation and were *n* type with 5 Ω cm of resistivity.

After the deposition, some of the SiN_x:H samples were rapid thermally annealed in Ar atmosphere at temperatures between 300 and 1050 °C for 30 s. This was done inside a graphite susceptor in a modular process technology RTP-600 furnace. After the annealing, each film for ESR measurements was cut in five smaller pieces of 0.2 cm×1 cm which were stacked to enhance the level of the detected microwave absorption. The ESR study was performed with a Bruker ESP 300E spectrometer operating in the *X* band at a microwave power of 0.5 mW. The density of Si dangling bonds (in the following, N_{db}) was quantified by comparison with the signal of a calibrated weak pitch standard. The measurements were carried out at room temperature.

The samples for electrical measurements underwent additional processing after the RTA cycles in order to fabricate the metal contacts. This was done by thermal evaporation of Al. The front contact was evaporated through a mask in order to produce several contacts of about 0.1 mm^2 of area on each sample, while no mask was used for the back contact. After evaporation of the Al, a postmetal anneal was performed at 300 °C for 20 min in a conventional furnace purged with Ar. Once finished, the MNS devices are characterized by measurements of the $C-V$ characteristics—high frequency (C_h) and quasistatic (C_q) curves. Both curves were measured simultaneously with a Keithley Model 82 system, and the distribution of interface charge traps (in the following, D_{it}) is obtained by means of the well-known equation[16]

$$D_{\mathrm{it}}=\frac{1}{q}C_{\mathrm{it}}=\frac{1}{q}\left[\left(\frac{1}{C_q}-\frac{1}{C_{\mathrm{diel}}}\right)^{-1}-\left(\frac{1}{C_h}-\frac{1}{C_{\mathrm{diel}}}\right)^{-1}\right], \quad (1)$$

where q is the electron charge and C_{diel} is the dielectric capacitance measured in accumulation.

The MNS devices were also characterized by current–voltage ($I-V$) measurements in accumulation using the same Keithley Model 82 equipment. This allowed the calculation of the resistivity (ρ) in the region of ohmic conduction, where proportionality exists between current and voltage. From these measurements, we also obtain the breakdown field (E_B), defined as the electric field that produces a sudden and abrupt increase of current conduction through the dielectric. In the high voltage region of the measurements, we observe a Poole–Frenkel conduction process in all the analyzed devices.[12,13]

As we will discuss in the following sections, the deterioration of the electrical properties for annealing temperatures above a certain threshold is associated to the processes of hydrogen release. In our previous studies[30] we determined the content of hydrogen in the films from the infrared absorption bands corresponding to the N–H and Si–H bonds. For this purpose, we used the oscillator strengths originally calibrated by Lanford and Rand.[31] However, it is well known that a significant amount of atomic or molecular hydrogen can be trapped in microvoids[32,33] of the SiN_x:H lattice. In our films, the evidence for this nonbonded hydrogen became clear when a significant increase of the IR absorption areas was observed at moderate annealing temperatures. Such increase indicated the formation of Si–H and N–H groups from dangling bonds and a fraction of the nonbonded hydrogen. Therefore, it was appropriate to utilize a detection procedure that is not sensitive to the chemical state of the hydrogen atoms, but instead it can detect the total amount of hydrogen irrespective of their bonding configuration. This was achieved by heavy ion elastic recoil detection analysis (HIERDA) performed at the Ionen Strahl Laboratorium of the Hahn-Meitner-Institut in Berlin. For these measurements we used ^{86}Kr incident ions accelerated at 1.4 MeV/amu. A comparatively high detection sensitivity achieved by an improved detection system with a solid angle of 0.4 msr and the use of a large detection angle of 40° provided a reasonable measuring statistics even at low ion fluences. The total ion dose was about 10^{12} particles per sample. The mass and energy dispersive time-of-flight setup is described in detail in Ref. 34.

III. RESULTS

A. E_B and ρ values

The values of E_B and ρ for the three series of analyzed samples are plotted in Figs. 1(a) and 1(b), respectively, versus the temperature of the RTA. The best electrical properties are those of the N-rich films, which have the higher values of ρ and E_B and the better thermal stability.[35] The deterioration of their characteristics takes place above 600 °C, compared to 400–500 °C for the near stoichiometric samples and 400 °C for the Si-rich composition. Although the deterioration of the near stoichiometric films begins at 400 °C for ρ and 500 °C for E_B, good values are maintained up to 600 °C. Above this temperature the deterioration process sharply arises.

B. Density of paramagnetic dangling bonds

In Fig. 2, we present N_{db} as a function of the RTA temperature. In all cases the signal corresponds to Si dangling bonds. After a significant reduction by more than one order of magnitude of the N_{db} concentration, this trend is reversed above 600 °C for both the N-rich and near stoichiometric films. In the Si-rich case, this onset is situated at 400 °C and the initial decrease is much less significant. Regarding both Figs. 1 and 2, it seems that the processes responsible for the

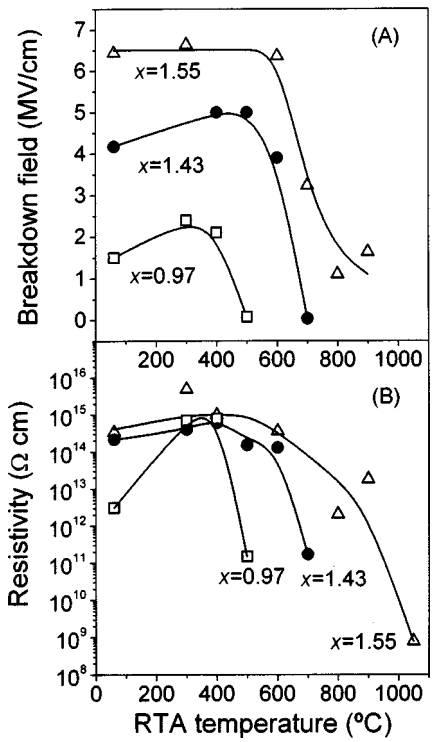

FIG. 1. (a) Breakdown field vs temperature of the rapid thermal annealing processes for the Si-rich ($x=0.97$), near stoichiometric ($x=1.43$), and N-rich films ($x=1.55$). (b) Resistivity of the three types of films analyzed in this study is plotted as a function of annealing temperature. The lines are a guide for the eye in both cases.

deterioration of the electrical properties and for the increase of the N_{db} density should be discussed together. This will be done in the next section.

With regard to the initial decrease of N_{db} at moderate temperatures, we showed in a previous publication[36] that it was not possible to relate this effect to bond formation reactions that could be detected in the infrared spectra. This led us to conclude that the observed behavior was a consequence of the negative correlation energy[37,38] of this defect. In fact, the combination of one positively and one negatively charged diamagnetic state is more stable than two neutral

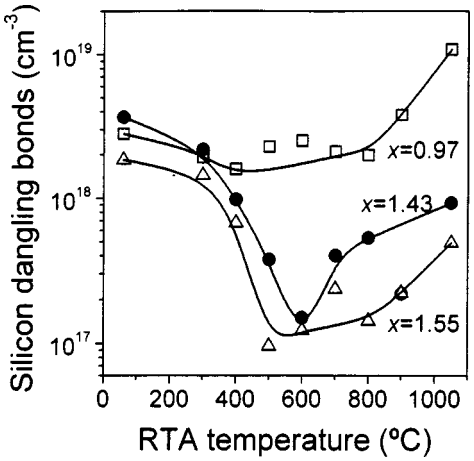

FIG. 2. Density of silicon dangling bonds as a function of RTA temperature. Lines are guides for the eye.

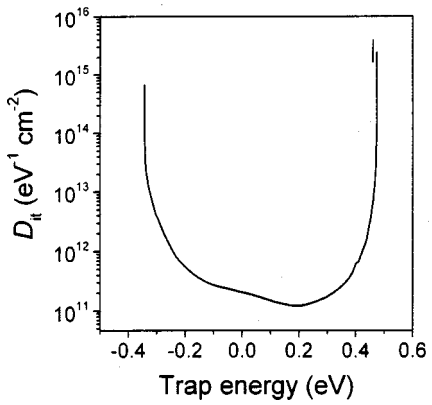

FIG. 3. Distribution of the density of interface states within the band gap of the semiconductor vs energy referred to midgap.

paramagnetic states. Therefore, the influence of the temperature favors the conversion of paramagnetic to diamagnetic (and hence ESR undetectable) states. For the Si-rich case, the significant reduction of the optical gap reduces the differences between the energy of diamagnetic and paramagnetic states, and it has been reported that the correlation energy may even become positive.[37] In that case, the conversion of paramagnetic to diamagnetic defects is no longer an energetically favored process, in accordance with the less significant variation of the N_{db} density for the $x=0.97$ samples. In this article, we will examine more closely these results in conjunction with the density of interface and band tail states to show that other effects may also be involved in the $x=1.43$ and $x=1.55$ films.

C. Interface trap density

In Fig. 3, we present the D_{it} of a sample with an as grown composition of $x=1.43$. The *U* shape of the distribution is determined by the band tails of the silicon nitride. The states that constitute the band tails originate mainly from stretched and distorted Si–Si bonds and have an extended nature. On the contrary, broken silicon bonds produce silicon dangling bonds which form localized states within the band gap at an energy that depends on the atoms that are back-bonded to the silicon atom.[25] In addition, the resulting *U*-shaped distribution is asymmetrical, being its minimum shifted to a value above midgap. This is due to the fact that the SiN_x:H valence band tail is always larger than the conduction band tail, which remains relatively unaffected by topological disorder.[39]

In Figs. 4(a) and 4(b) we plot the minimum of D_{it} and the energy position of that minimum versus the RTA temperature. A clear parallelism appears between the trends of the two parameters. This is indicative that the variations in D_{it} are associated mainly with centers with energy in the lower half of the semiconductor gap, such as band tail states of the SiN_x:H valence band in the region next to the interface. The reduction of the density of states in the gap is expected to be parallel to a shift of the minimum of the D_{it} distribution towards midgap. This should be due to the

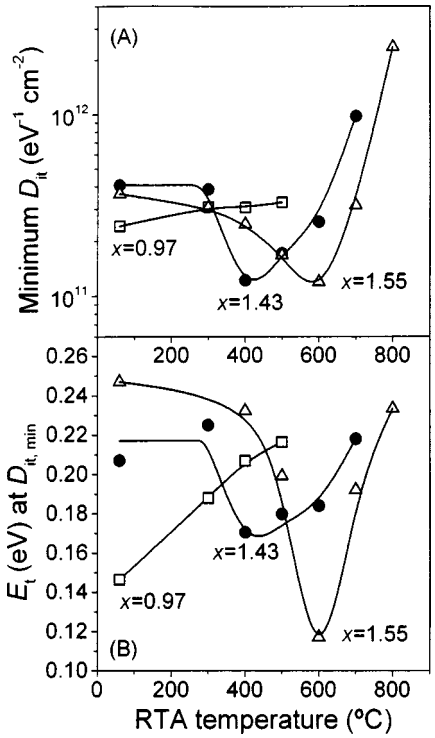

FIG. 4. (a) Values of the minimum of the distribution of interface states within the gap of the semiconductor. The data have been plotted vs the temperature of the RTA process. (b) Trap energy (E_t), referred to midgap, at the minimum of the distribution of interface states. Lines are drawn as guides for the eye in both figures.

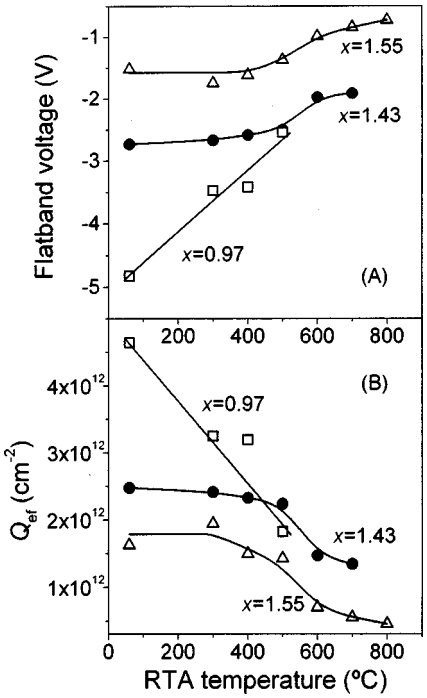

FIG. 5. (a) Plot of the voltage that produces the situation of flat bands at the semiconductor surface vs the temperature of the annealing treatments for the three compositions analyzed in this study. (b) Density of effective charge in the dielectric as a function of annealing temperature. Lines are guides for the eye in both figures.

amount of topological disorder being reduced by the thermal relaxation processes that take place at moderate RTA temperatures.

A qualitatively different behavior is observed for the Si-rich films compared to the near stoichiometric and N-rich samples. In these latter ones, a significant reduction of the minimum of D_{it} is observed at moderate annealing temperatures (up to 600 °C for the N-rich films and 400 °C for the near stoichiometric). On the other hand, in the Si-rich samples, no such reduction takes place and the minimum of D_{it} increases in the whole range of temperatures in which the quasistatic capacitance can be measured.

A similar behavior of the Si-rich films has been observed in Ref. 40 for the optical coefficients that account for the disorder of the SiN_x:H lattice as it is observed in the optical absorption edge (Urbach energy, E_0, and Tauc parameter, B). These parameters revealed that a thermal relaxation of the network strain took place at moderate annealing temperatures for the near stoichiometric and N-rich compositions, but not for the Si rich. This was attributed to the higher rigidity of the Si-rich lattice, which has a high number of bonding constraints caused by the higher coordination number of silicon compared to nitrogen. The same factor impedes any thermal relaxation taking place for the interface states of the Si-rich composition, and causes the rapid deterioration of its electrical properties.

D. Effective electric charge

In Figs. 5(a) and 5(b) we plot the flatband voltage and the density of effective charge versus the temperature of the RTA treatment for the three compositions. Both parameters indicate a gradual disappearance of the charge stored in the dielectric as the temperature of the annealing processes is increased. The voltage corresponding to flat band conditions shifts towards the value of the Al/Si work-function difference (-0.60 ± 0.05 V), but only in the N-rich series gets close to this value. This is an indication of an almost complete disappearance of stored charge only in this case. The effective dielectric charge is larger in the Si-rich case and lower for the N-rich composition. This seems to indicate that the microscopic origin of this charge is predominantly associated with silicon centers, such as positively charged Si dangling bonds resulting from incomplete reaction of silane fragments during the growth process. Comparing with the minimum of D_{it} [Fig. 4(a)] and N_{db} (Fig. 2), we see that their behavior as a function of RTA temperature is completely different. While the effective charge tends to disappear at high annealing temperatures, the minimum of D_{it} and N_{db} follow U-shaped trends for the near stoichiometric and N-rich samples, that is to say, for compositions above the percolation threshold (fixed in SiN_x:H films at a composition $x=1.1$).[39] This suggests that the hydrogen release processes affect the disorder of the structure (tail states such as weak or stretched Si–Si bonds) and the dangling bond density. On the contrary, the net charge is not affected but is gradually compensated by injection of electrons upon the annealing.

Given the negligible contribution that the interface states have in the effective charge,[41] it is assumed that the polarization has no influence on this charge. However, some degree of clockwise hysteresis of the high frequency capacitance exists, indicating that slow traps capture holes in the

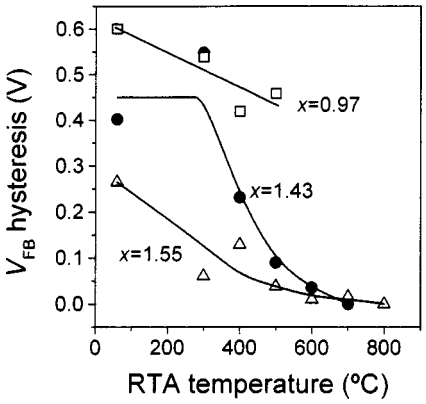

FIG. 6. Evolution of the hysteresis of the high frequency capacitance curve quantified as the shift of the voltage necessary to achieve the flatband condition (V_{FB}). Lines are drawn as a guide for the eye.

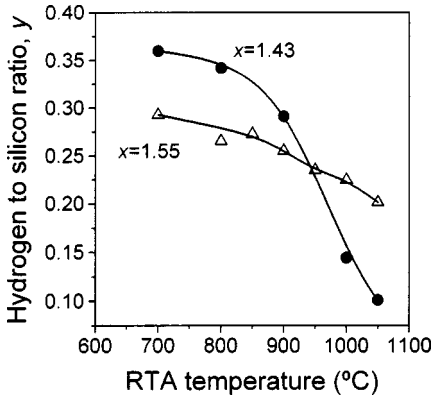

FIG. 7. Ratio of hydrogen to silicon ($y=[H]/[Si]$) in the near-stoichiometric ($x=1.43$) and N-rich films ($x=1.55$). It was calculated from the atomic percents of each element determined by HIERDA, only in the range of high annealing temperatures. Lines are guides for the eye.

sweep from accumulation to inversion. In Fig. 6, we have plotted the hysteresis versus the RTA temperature. It has been measured as the shift of the flatband voltage between two consecutive sweeps from accumulation to inversion and vice versa. It can be seen that, in much the same way as the effective charge, the hysteresis disappears gradually with the annealing temperature. The larger values correspond again to the Si-rich composition, and the lower ones to the N-rich films. For annealing temperatures above 500 °C, the hysteresis disappears almost completely for the samples of the N-rich and near stoichiometric composition. For these two series, the decrease of the hysteresis is faster than for the net dielectric charge, indicating that the trapped charges that can interchange charge with the semiconductor disappear before the fixed charge.

IV. DISCUSSION

We will center our discussion in the following points:

(i) The rapid deterioration of the electrical properties above 600 °C for the N-rich and near stoichiometric samples: see Figs. 1(a) and 1(b) (E_B and ρ), Fig. 2 (N_{db}), and Fig. 4(a) (minimum of D_{it}). The only exception to this seems to be the behavior of the minimum of D_{it} for the near stoichiometric samples, which increases above 400 °C instead of 600 °C. In addition, the deterioration of ρ for this series begins at 400 °C, and at 500 °C for E_B, but the decreasing trend for these two parameters is more pronounced above 600 °C.

(ii) The mechanisms responsible for the decrease of the minimum of D_{it} and N_{db} at moderate annealing temperatures for the N-rich and near stoichiometric samples.

(iii) The peculiar case of the Si-rich samples, which are the only series with a composition below the percolation threshold of Si–Si bonds in the SiN_x:H lattice, and therefore characterized by the rigidity caused by the chains of tetracoordinated Si atoms. In these samples, the electrical properties deteriorate above 400 °C, except for the minimum of D_{it} which increases continuously in the whole range of temperatures. Additionally, the initial decrease of N_{db} is much less significant than for the two other series.

(iv) The gradual disappearance of both the effective charge and the hysteresis when increasing the annealing temperature for all the three series of samples analyzed, in contrast with the *U*-shaped behavior of the trends of N_{db} and the minimum of D_{it}.

We begin with the first of the above discussion points, that is to say, the deterioration of the electrical properties above 600 °C for the near stoichiometric and N-rich films. From the data of Table I relative to composition and bonding arrangement, and other data that supported them, we proposed in previous publications a set of chemical bond reactions that explained the observed results.[30,40] For the near stoichiometric samples, the loss of nitrogen and bonded hydrogen above 700 °C was modeled by an interaction between Si–H bonds and nearby N atoms of N–H groups. The consequence is the effusion of ammonia fragments and the formation of weak Si-Si bonds between the broken silicon bonds that result from this process.[30,40]

In the N-rich case, no Si–H bonds were detected in the infrared spectra and therefore the process of hydrogen release cannot be the same as for the near stoichiometric samples. The N-rich films do not loose N atoms at any annealing temperature, showing a better thermal stability.[35] The loss of bonded hydrogen takes place mainly above 900 °C by the interaction of nearby N–H groups with the effusion of a hydrogen molecule. However, at temperatures lower than this 900 °C, part of the nonbonded hydrogen trapped in microvoids of the structure may be escaping from the sample. This leaves empty cavities that produce an increase of the surface to volume ratio of the film and therefore an increase of current conduction through the dielectric, explaining the decrease of both ρ and E_B.[35]

Following with the discussion, in Fig. 7 we plot the hydrogen to silicon ratio in the near stoichiometric and N-rich samples, obtained from the atomic concentrations determined by HIERDA.[42] Only the range of high annealing temperatures was investigated by this technique. The release of hydrogen in this range of annealing temperatures becomes clearly apparent in this figure. Thus, it seems reasonable to associate this process with the deterioration of the electrical properties. The first to escape would be the nonbonded fraction of the hydrogen trapped in the film. When these hydrogen atoms and molecules leave the film, empty microvoids

are left behind, whose unpassivated internal surfaces constitute easy paths of current conduction across the dielectric. Next, the bonded hydrogen leaves the films by means of the chemical bond reactions that have been proposed in Refs. 30 and 40. These reactions produce weak Si–Si bonds and dangling bonds, explaining the sharp deterioration of the electrical characteristics at the highest RTA temperatures. In fact, the quasistatic capacitance can not be measured above 700 °C for the near stoichiometric films, and above 800 °C for the N-rich ones, due to leakage currents in the SiN_x:H.

We now go on to point (ii) of our discussion, that is to say, the decrease at moderate temperatures of N_{db} (Fig. 2) and the minimum of D_{it} [Fig. 4(a)] for the N-rich and near stoichiometric samples. We explain these results as follows: The results of Figs. 4(a) and 4(b) indicate a strong parallelism between both set of data which suggests that the reduction of the density of D_{it} at moderate annealing temperatures is mainly due to a decrease of states in the valence band tail of the SiN_x:H. In fact, from Fig. 3, the distribution of D_{it} is dominated by states in the lower half of the band gap and their shape seems to be more likely due to band tail extended states rather than localized groups of defects, which would have given rise to peaks in the spectra. In the case of the SiN_x:H, the band tail states are mainly due to Si–Si bonds that are weakened by strain and distortions in the bond angles. Above a certain threshold energy, those states may convert into Si dangling bond centers which would give rise to localized states situated at about midgap, so that the reduction of band tail states observed in the D_{it} distributions would result in a reduction of N_{db}, as Figs. 4(a) and 2 indicate, respectively.

In support of this model we can present an additional result, which is the comparison of N_{db} with the Urbach energy E_0, for the particular case of the near stoichiometric composition. As it is known,[40] the Urbach energy is the inverse of the slope of the exponential absorption edge of the optical absorption coefficient (α). The larger the disorder of the amorphous network, the lower will be the slope of the absorption edge. This is due to the strain and disorder of the weak bonds becoming more significant, since these bonds will give rise to states that extend deeper into the gap. Because the Urbach energy is the inverse of the exponential band tail, E_0 will be a parameter proportional to the disorder, and because of the relation between weak bonds and dangling bonds, it should be proportional to the N_{db} density. Figure 8 shows that this proportionality exists for the near stoichiometric samples. That is to say, both N_{db} and the Urbach energy have *U*-shaped trends as a function of the RTA temperature, with a minimum at 600 °C. A detailed analysis of the optical absorption properties of our SiN_x:H films can be found in Ref. 40.

Our next point of discussion (iii) is the peculiar behavior of the Si-rich samples, in the sense that the trends of some parameters with the annealing temperature are different than for the near stoichiometric and N-rich series. Particularly, the minimum of D_{it} does not show a *U*-shaped trend as a function of the RTA temperature. On the contrary, it increases steadily from the lower annealing temperatures until the leakage current is so high that the quasistatic capacitance can no longer be measured (above 500 °C). Both ρ and E_B decrease from 400 °C, and N_{db} increases above the same temperature. The sharp increase of the leakage current above 500 °C is due to the effusion of hydrogen molecules from near Si–H groups, that initiates the decrease of the content of bonded hydrogen[43]

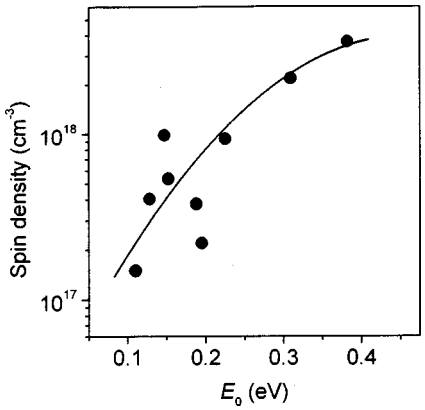

FIG. 8. Proportionality between the Si dangling bond density (spin density) and the Urbach energy parameter (E_0) obtained from the optical absorption edge. The data points correspond to the near stoichiometric series ($x = 1.43$) in the whole range of annealing temperatures. The line is a guide for the eye.

$$\text{Si–H}+\text{Si–H}\rightarrow \text{H}_2\uparrow+\text{Si–Si}. \tag{2}$$

This process only occurs in the Si-rich samples and is due to the significantly higher concentration of Si–H bonds that these samples have, probably due to an incomplete reaction of silane molecules during the growth process. We will explain this point in detail in the next paragraphs.

In the near stoichiometric samples, the release of hydrogen only occurs simultaneously with the loss of nitrogen above 700 °C according to the bond reaction described in Refs. 30 and 40

$$\text{Si–H}+\text{H–NSi–H}\rightarrow \text{Si–Si}+\text{NH}_3\uparrow, \tag{3}$$

while in the Si-rich case this process of simultaneous loss of nitrogen and hydrogen occurs above 600 °C (see Table I). Then, the process described by Eq. (2) anticipates the electrical deterioration process of the Si-rich films with respect to the near stoichiometric ones.

Another factor that has an important influence is the percolation of chains of Si–Si bonds along the dielectric lattice. The percolation threshold for these chains is located at a value of $x = 1.1$ (see Ref. 39 for details). Our Si-rich samples have an as-grown value of $x = 0.97$ (see Table I). This means a silicon content higher than the threshold, so percolation exists. On the other hand, for the near stoichiometric films, the value of x is 1.43 which indicates a silicon content lower than the threshold and no percolation occurs. Because of the high coordination number of silicon (4), the average number of constraints is increased with the silicon content, and the percolation of Si–Si bonds results in a rigid and strained structure. Consequently, the Si-rich films do not experience the thermal relaxation processes of the bonding configurations, which are characteristic of the other types of films at moderate annealing temperatures. This can be clearly seen in

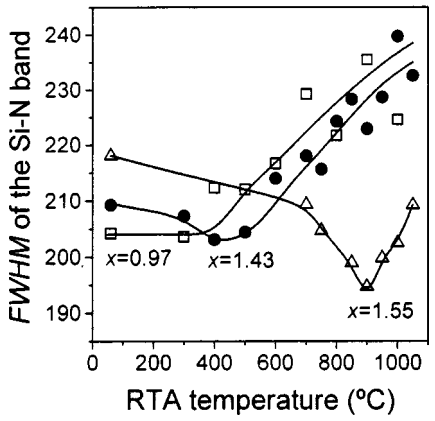

FIG. 9. Full width at half maximum of the Si–N infrared absorption band for the three types of samples analyzed. Lines are drawn to guide the eye.

Fig. 9, where we plot the full width at half maximum (FWHM) of the absorption band of the Si–N bonds in the infrared spectra (see Ref. 40). A narrower band means lower dispersion of bond angles and lengths, and therefore a more ordered structure. While the N-rich and near stoichiometric samples experience a decrease of the FWHM parameter at moderate annealing temperatures, indicating a thermal relaxation of bonding strains and distortions, the Si-rich samples do not experience this initial decrease of FWHM. This supports the hypothesis that the percolation of rigidity caused by the Si–Si bonds prevents the thermal relaxation processes, and explains why in these films the annealing treatments at moderate temperatures cause a general deterioration above 400 °C.

Regarding our last point of discussion (iv), we first remark that the very different trends of the dielectric effective charge [Fig. 5(b)] and the flat band hysteresis (Fig. 6) with respect to the minimum of D_{it} [Fig. 4(a)] indicate a completely different microscopic origin of the defects that cause each of them. Both the dielectric charge and the hysteresis of the high frequency capacitance decrease gradually when the temperature of the annealing treatments is increased. Moreover, in the case of the N-rich films the shift of the flat band voltage [Fig. 5(a)] is reduced almost to the difference of work functions between the aluminum contact and the silicon substrate at the higher annealing temperature. The hysteresis of the flat band voltage decreases faster than the amount of stored charge and it almost disappears for annealing temperatures above 500 °C in the N-rich and near stoichiometric samples. Particularly, in the Si-rich case, the hysteresis is significant in the whole range of temperatures. This seems to suggest that the contribution of interface states to the shift of the flat band voltage is negligible and the dielectric charge is then dominated by bulk defects. As can be seen in Figs. 5(b) and 6, the density of stored charge and the hysteresis are lower for the N-rich films compared to the Si-rich samples. The higher values of both parameters for the Si-rich films are tentatively associated to partially dissociated silane molecules that are trapped in the network in charged states during the growth process. As the temperature of the annealing processes increases these excited species are incorporated to the SiN_x:H lattice and progressively lose their charge. The small hysteresis of the high frequency capacitance curve would then be caused by the fraction of these charges located near the semiconductor surface and therefore able to interchange charge with it.

V. CONCLUSIONS

We have analyzed the electrical properties of SiN_x:H films by $C-V$ and $I-V$ measurements in MNS structures as a function of the RTA temperature. We emphasize the crucial role that the hydrogen content has in determining the behavior of the dielectric. For this purpose, the total content of hydrogen was determined by HIERDA analysis. The results have been compared with the N_{db} determined by ESR measurements and discussed in the context of previous studies of composition and bonding structure by RBS/EDX and infrared spectroscopy. It was found that the response of the dielectric to the thermal treatments is essentially determined by its as-grown composition being above or below the percolation threshold ($x=1.1$) of Si–Si bonds in the SiN_x:H lattice.

Three types of films have been investigated: two with their as-grown composition above the percolation threshold (N-rich as-grown composition $x=1.55$; near stoichiometric, as-grown composition $x=1.43$), and the other one with an as-grown composition below the percolation threshold and referred to as Si rich ($x=0.97$).

In the N-rich and near stoichiometric cases, the density of N_{db} and the minimum of D_{it} experience a significant decrease up to an intermediate annealing temperature. The thermal relaxation of the strain of the SiN_x:H lattice at moderate annealing temperatures produces a significant decrease of the density of interface states. On the contrary, the rigidity of the Si-rich structure impedes this relaxation process, and the minimum of D_{it} increases in this case from the lower annealing temperatures. Since a relation exists between the density of weak Si–Si and Si–N bonds and the density of Si dangling bonds, the relaxation of the strain of the former will also reduce the density of the latter. This explains the behavior of N_{db} with the RTA temperature.

For higher annealing temperatures, the release of hydrogen trapped in microvoids of the structure will initiate the degradation of the electrical characteristics by leaving behind unpassivated internal surfaces. As a consequence, both ρ and E_B decrease, and the leakage current through the dielectric increases. The SiN_x:H network is damaged by this process and the minimum of D_{it} and N_{db} increase. The analysis of the hydrogen content by HIERDA has confirmed clearly the hydrogen release in the range of high temperatures of annealing.

In the Si-rich case, the percolation of rigidity through the network impedes the relaxation processes and anticipates the degradation phenomena to lower temperatures. Compared to the near stoichiometric case, an additional process of hydrogen release consisting on the interaction between near Si–H bonds also contributes to initiate the deterioration of the electrical characteristics at lower temperatures.

The density of effective charge stored in the SiN_x:H has a different microscopic origin than the interface states. The effective charge disappears as the temperature of the RTA

treatments is increased, while the density of interface states increases in the high temperature range. As both the shift of the flat band voltage and the hysteresis are significantly higher for the Si-rich films, we have proposed that most of the stored charge is located at silicon centers formed by charged fragments of silane molecules during the deposition process.

ACKNOWLEDGMENTS

The authors wish to express our gratitude to Dr. W. Bohne, Dr. J. Röhrich, and Dr. B. Selle, from the Hahn-Meitner-Institut in Berlin, for a long friendship and fruitful collaboration, from which the HIERDA results presented in this work are only a small part. They also thank the financial support of the Spanish National Office for Science and Technology under Grant No. TIC98/0740 and the technical assistance received from the ion implantation facility ''CAI-Implantación Iónica'' of the University of Madrid.

[1] J. Kanicki, F. R. Libsch, J. Griffith, and R. Polastre, J. Appl. Phys. **69**, 2339 (1991).
[2] H. C. Cheng, H. W. Liu, H. P. Su, and G. Hong, IEEE Electron Device Lett. **16**, 509 (1995).
[3] J. Schmidt and A. G. Aberle, J. Appl. Phys. **85**, 3626 (1999).
[4] Y. Wu and G. Lucovsky, IEEE Electron Device Lett. **19**, 367 (1998).
[5] W. Lu, X. W. Wang, R. Hammond, A. Kuliev, S. Koester, J. O. Chu, K. Ismail, T. P. Ma, and I. Adesida, IEEE Electron Device Lett. **20**, 514 (1999).
[6] H. Y. Yang, H. Niimi, and G. Lucovsky, J. Appl. Phys. **83**, 2327 (1998).
[7] Y. Wu, Y. Lee, and G. Lucovsky, IEEE Electron Device Lett. **21**, 116 (2000).
[8] D. T. Krick, P. M. Lenahan, and J. Kanicki, Phys. Rev. B **38**, 8226 (1988).
[9] W. L. Warren, J. Kanicki, J. Robertson, E. H. Poindexter, and P. J. McWhorter, J. Appl. Phys. **74**, 4034 (1993).
[10] W. Warren, P. M. Lenahan, and S. E. Curry, Phys. Rev. Lett. **65**, 207 (1990).
[11] W. L. Warren, J. Kanicki, J. Robertson, and P. M. Lenahan, Appl. Phys. Lett. **59**, 1699 (1991).
[12] M. C. Hugon, F. Delmotte, B. Agius, and J. L. Courant, J. Vac. Sci. Technol. A **15**, 3143 (1997).
[13] M. Tao, D. Park, N. Mohammad, D. Li, A. Botchkerav, and H. Morkoc, Philos. Mag. B **73**, 723 (1996).
[14] D. Landheer, K. Rajesh, D. Masson, J. E. Hulse, G. I. Sproule, and T. Quance, J. Vac. Sci. Technol. A **16**, 2931 (1998).
[15] S. C. Witczak, J. S. Suehle, and M. Gaitan, Solid-State Electron. **35**, 345 (1992).
[16] E. H. Nicollian and J. R. Brews, *MOS (Metal–Oxide–Semiconductor) Physics and Technology* (Wiley, New York, 1982).
[17] E. H. Nicollian and A. Goetzberger, Bell Syst. Tech. J. **46**, 1055 (1967).
[18] G. Lucovsky, Y. Wu, H. Niimi, V. Misra, and J. C. Phillips, Appl. Phys. Lett. **74**, 2005 (1999).
[19] S. Garcia, I. Martil, G. Gonzalez Diaz, E. Castan, S. Dueñas, and M. Fernandez, J. Appl. Phys. **83**, 332 (1998).
[20] A. Kapila and V. Malhotra, Appl. Phys. Lett. **62**, 1009 (1993).
[21] K. Vaccaro, H. M. Dauplaise, A. Davis, S. M. Spaziani, and J. P. Lorenzo, Appl. Phys. Lett. **87**, 527 (1995).
[22] D. G. Park, J. C. Reed, and H. Morkoc, Appl. Phys. Lett. **71**, 1210 (1997).
[23] E. H. Poindexter, G. J. Gerardi, M. E. Rueckel, P. J. Caplan, N. M. Johnson, and D. K. Biegelsen, J. Appl. Phys. **56**, 2844 (1984).
[24] A. Stesmans, Semicond. Sci. Technol. **4**, 1000 (1989).
[25] D. Jousse, J. Kanicki, and J. H. Stathis, Appl. Phys. Lett. **54**, 1043 (1989).
[26] J. R. Elmiger and M. Kunst, Appl. Phys. Lett. **69**, 517 (1996).
[27] Z. Lu, S. S. He, Y. Ma, and G. Lucovsky, J. Non-Cryst. Solids **187**, 340 (1995).
[28] Z. Jing, G. Lucovsky, and J. L. Whitten, J. Vac. Sci. Technol. B **13**, 1613 (1995).
[29] Z. Lu, P. Santos-Filho, G. Stevens, M. J. Williams, and G. Lucovsky, J. Vac. Sci. Technol. A **13**, 607 (1995).
[30] F. L. Martínez, I. Mártil, G. González-Díaz, B. Selle, and I. Sieber, J. Non-Cryst. Solids **227–230**, 523 (1998).
[31] W. A. Lanford and M. J. Rand, J. Appl. Phys. **49**, 2473 (1978).
[32] R. E. Norberg, D. J. Leopold, and P. A. Fedders, J. Non-Cryst. Solids **227–230**, 124 (1998).
[33] H. J. Stein, S. M. Myers, and D. M. Follstaedt, J. Appl. Phys. **73**, 2755 (1993).
[34] W. Bohne, J. Röhrich, and G. Röschert, Nucl. Instrum. Methods Phys. Res. B **136–138**, 633 (1998).
[35] F. L. Martínez, A. del Prado, D. Bravo, F. López, I. Mártil, and G. González-Díaz, J. Vac. Sci. Technol. A **17**, 1280 (1999).
[36] F. L. Martínez, A. del Prado, I. Mártil, D. Bravo, and F. J. López, J. Appl. Phys. **88**, 2149 (2000).
[37] P. M. Lenahan, D. T. Krick, and J. Kanicki, Appl. Surf. Sci. **39**, 392 (1989).
[38] S. E. Curry, P. M. Lenahan, D. T. Krick, J. Kanicki, and C. T. Kirk, Appl. Phys. Lett. **56**, 1359 (1990).
[39] J. Robertson, Philos. Mag. B **63**, 47 (1991).
[40] F. L. Martínez, A. del Prado, I. Mártil, G. González-Díaz, B. Selle, and I. Sieber, J. Appl. Phys. **86**, 2055 (1999).
[41] Y. Ma, T. Yasuda, and G. Lucovsky, J. Vac. Sci. Technol. B **11**, 1533 (1993).
[42] W. Bohne, W. Fuhs, J. Röhrich, B. Selle, G. González Díaz, I. Mártil, F. L. Martinez, and A. del Prado, Surf. Interface Anal. **30**, 534 (2000).
[43] K. Zellama, L. Chahed, P. Slàdek, M. L. Théye, J. H. Von Bardeleben, and P. Roca i Cabarrocas, Phys. Rev. B **53**, 3804 (1996).